

# Decays $Z \rightarrow e_a e_b$ in a 3-3-1 model with neutral leptons

T.T. Hong,<sup>1,2,\*</sup> L. T. Hue,<sup>3,4,†</sup> L.T.T. Phuong,<sup>1,2,‡</sup>

N.H.T. Nha,<sup>3,4,§</sup> and T. Phong Nguyen <sup>¶5,\*\*</sup>

<sup>1</sup>*An Giang University, Long Xuyen City, Vietnam*

<sup>2</sup>*Vietnam National University, Ho Chi Minh City, Vietnam*

<sup>3</sup>*Subatomic Physics Research Group,*

*Science and Technology Advanced Institute,*

*Van Lang University, Ho Chi Minh City, Vietnam*

<sup>4</sup>*Faculty of Applied Technology, School of Technology,*

*Van Lang University, Ho Chi Minh City, Vietnam*

<sup>5</sup>*Department of Physics, Can Tho University, 3/2 Street, Can Tho, Vietnam*

## Abstract

We investigate the 3-3-1 model with neutral leptons, a specific extension of the 3-3-1 models that includes heavy neutral leptons, which are sufficient to accommodate the neutrino oscillation data via the inverse seesaw mechanism. We will point out that this model can simultaneously explain the lepton flavor violating decays of the  $Z$  and Standard Model-like Higgs bosons into different charged leptons  $Z, h \rightarrow e_a e_b$ , as well as the charged lepton decays  $e_b \rightarrow e_a \gamma$ , in agreement with the recent experimental data. In addition, the numerical results show strong correlations among the decay rates of the  $Z$  and  $h$  bosons predicted by this model. Specifically, some of these rates are nearly linearly dependent on each other. Consequently, the decay channels can be theoretically determined if one of them is detected in experiments.

PACS numbers:

---

<sup>¶</sup> Corresponding author

\*Electronic address: tthong@agu.edu.vn

†Electronic address: lethohue@vlu.edu.vn

‡Electronic address: ltphuong@agu.edu.vn

§Electronic address: nguyenuathanhnhha@vlu.edu.vn

\*\*Electronic address: thanhphong@ctu.edu.vn

## I. INTRODUCTION

We will use the results of the general one-loop contributions introduced recently [1] to the lepton flavor violating (LFV) decay amplitudes of the  $Z$  boson (LFV $Z$ ),  $Z \rightarrow e_a e_b$ , with  $e_a, e_b = e, \mu, \tau$  and  $e_a \neq e_b$ , to study an extension of the 3-3-1 model adding neutral leptons as  $SU(3)_L$  singlets (331 $NL$ ) to accommodate the neutrino oscillation data through the inverse seesaw (ISS) mechanism [2]. The 3-3-1 models were constructed based on the gauge group  $SU(3)_C \otimes SU(3)_L \otimes U(1)_X$  [3–7], providing an interesting explanation for the existence three fermion families based on the anomaly-free requirements in the fermion sector [5]. Normally, all left-handed fermions in the SM doublets are included in the respective  $SU(3)_L$  triplets or antitriplets of the 3-3-1 models. The leptons with certain electric charges in the third component of the lepton  $SU(3)_L$  (anti) triplets are used to distinguish different 3-3-1 models. The 3-3-1 models with arbitrary electric charges for these new leptons were also introduced [8–10]. The 331 $NL$  model discussed here consists of three neutral left-handed leptons in the third component of the three lepton triplets. Therefore, three other neutral lepton  $SU(3)_L$  singlets are sufficient for generating active neutrino masses and mixing parameters through the ISS mechanism. It has been shown that if all heavy ISS neutrino masses are degenerate, the strong correlations between the three cLFV decay rates (branching ratios)  $\text{Br}(e_b \rightarrow e_a \gamma)$  will predict invisible signals of the two decays  $\tau \rightarrow \gamma e, \gamma \mu$  in the near future [2]. In contrast, the model with non-degenerate masses of heavy neutrinos will predict large decay rates for the cLFV and LFV decays of the SM-like Higgs boson (LFV $h$ )  $h \rightarrow e\tau, \mu\tau$ , which can reach values of  $\mathcal{O}(10^{-4})$  [11]. In this work, we consider the more general situation of heavy ISS neutrinos having non-degenerate masses, so that all cLFV decay rates will reach recent and future experimental sensitivities. More interestingly, two processes, LFV $Z$  and LFV $h$  decays, will be discussed simultaneously to guarantee whether their decay rates are excluded, invisible, or still promising for search in upcoming experiments, see a summary in Table I.

LFV $Z$  decays have been investigated in many Beyond the Standard Models (BSM), predicting large LFV $Z$  but small LFV $h$  decay rates compared to upcoming experimental sensitivities. For example, it was shown that  $\text{Br}(Z \rightarrow \mu^\mp \tau^\pm) \propto \mathcal{O}(10^{-5})$ , and  $\text{Br}(h \rightarrow \mu^\mp e^\pm) \propto \mathcal{O}(10^{-11})$  in a simple SM extension adding only ISS neutrinos [12]. Similarly, a recent discussion on a Two-Higgs Doublet Model (2HDM) with ISS neutrinos predicts the large  $\text{Br}(Z \rightarrow \mu^\pm \tau^\mp) \propto \mathcal{O}(10^{-8})$  but suppressed values of  $\text{Br}(h \rightarrow \mu^\pm e^\mp) < 10^{-8}$

	Br	Latest experiment	Future sensitivity
cLFV	$\text{Br}(\mu \rightarrow e\gamma)$	$< 4.2 \times 10^{-13}$ [13–15]	$< 6 \times 10^{-14}$ [17, 18]
	$\text{Br}(\tau \rightarrow \mu\gamma)$	$< 4.4 \times 10^{-8}$ [13, 14, 16]	$< 6.9 \times 10^{-9}$ [17, 18]
	$\text{Br}(\tau \rightarrow e\gamma)$	$< 3.3 \times 10^{-8}$ [13, 14, 16]	$< 9.0 \times 10^{-9}$ [17, 18]
LFVh	$\text{Br}(h \rightarrow \mu^\pm e^\mp)$	$< 6.1 \times 10^{-5}$ [19]	$\sim \mathcal{O}(10^{-5})$ [21]
	$\text{Br}(h \rightarrow \tau^\pm \mu^\mp)$	$< 1.5 \times 10^{-3}$ [20]	$\sim \mathcal{O}(10^{-4})$ [21–23]
	$\text{Br}(h \rightarrow \tau^\pm e^\mp)$	$< 2.2 \times 10^{-3}$ [20]	$\sim \mathcal{O}(10^{-4})$ [21]
LFVZ	$\text{Br}(Z \rightarrow \mu^\pm e^\mp)$	$< 2.62 \times 10^{-7}$ [24]	$\sim 7 \times 10^{-8}$ (HL-LHC) and $10^{-10}$ (FCC-ee) [25–27]
	$\text{Br}(Z \rightarrow \tau^\pm \mu^\mp)$	$< 6.5 \times 10^{-6}$ [25]	$\sim 10^{-6}$ (HL-LHC) and $10^{-9}$ (FCC-ee) [26, 27]
	$\text{Br}(Z \rightarrow \tau^\pm e^\mp)$	$< 5.0 \times 10^{-6}$ [25]	$\sim 10^{-6}$ (HL-LHC) and $10^{-9}$ (FCC-ee) [26, 27]

TABLE I: The latest and expected experimental sensitivities on the LFV branching ratios (Br).

[28] in the regions of parameter space accommodating the  $(g - 2)_{e,\mu}$  data. When ignoring the  $(g - 2)_{e_a}$  anomalies, another investigation on a 2HDM with standard seesaw neutrinos predicts promising signals of LFVh, but the LFVZ decay rates are suppressed to be observed experimentally [29]. This implies that combined results from experimental searches for these two LFVh and Z decays may provide useful information to determine the reality of available BSM models. Therefore, LFVZ decays are attractive objects for both theoretical studies [1, 28–31] and experimental searches [32–34]. In conclusion, studying LFVZ decays is necessary for the 331NL model to see whether they are the strictest constraint among the three classes of LFV decay rates we focus on in this work.

The structure of this work is organized as follows. In section II, we will review the necessary components of the 331NL model for studying the  $Z \rightarrow e_a e_b$  decays and how the ISS framework can produce the active neutrino masses and mixing parameters consistent with the experimental data. We will also discuss the one-loop contributions to the decay amplitudes  $Z \rightarrow e_b e_a$ . The couplings and analytic formulas related to the LFVZ decays will be determined in section III. In section IV, we will numerically investigate three classes of cLFV, LFVZ, and LFVh decays, working out the allowed regions of the parameter space satisfying all LFV experimental limits. In section V, crucial results will be summarized and presented in our conclusions. Finally, Appendix A shows the master functions of the one-loop contribution to LFVZ decay amplitudes in the unitary gauge.

## II. THE 3-3-1 MODEL WITH NEUTRAL LEPTON

### A. Particle content and neutrino masses from the ISS mechanism

The 331NL model is a specific version of the 3-3-1 models, featuring new neutral leptons in the third component of the left-handed lepton triplets. We focus solely on particle spectrum of the 331NL model relevant to this work. In the 331NL model, the electric charge operator  $Q = T_3 - \frac{T_8}{\sqrt{3}} + X$  is identified by the gauge group  $SU(3)_L \times U(1)_X$ , in which  $T_{3,8}$  are diagonal  $SU(3)_L$  generators. Each lepton generation contains a  $SU(3)_L$  triplet  $L_a = (\nu_a, e_a, N_a)_L^T \sim (3, -\frac{1}{3})$ , a RH (right-handed) charged lepton  $e_{aR} \sim (1, -1)$ , and a new neutral lepton  $X_{aR} \sim (1, 0)$  with  $a = 1, 2, 3$ . The three Higgs triplets of the model are  $\rho = (\rho_1^+, \rho^0, \rho_2^+)^T \sim (3, \frac{2}{3})$ ,  $\eta = (\eta_1^0, \eta^-, \eta_2^0)^T \sim (3, -\frac{1}{3})$ , and  $\chi = (\chi_1^0, \chi^-, \chi_2^0)^T \sim (3, -\frac{1}{3})$ . All quark and lepton masses at tree-level are generated by the vacuum expectation values (vev) are  $\langle \rho \rangle = (0, \frac{v_1}{\sqrt{2}}, 0)^T$ ,  $\langle \eta \rangle = (\frac{v_2}{\sqrt{2}}, 0, 0)^T$  and  $\langle \chi \rangle = (0, 0, \frac{w}{\sqrt{2}})^T$ . Two neutral Higgs components have zero vevs due to they have non-zero lepton numbers [35], when the 331NL model respects a global symmetry  $U(1)_L$  defined as the generalized lepton number  $L$  that relates to the normal lepton number by  $L = \frac{4}{\sqrt{3}}T_8 + L$  [36]. Here, we explain more precisely that the two triplets  $\eta$  and  $\chi$  have the same quantum numbers of the total gauge group, but their values of the  $L$  assignments are different. Therefore, they have different Yukawa couplings and vevs, as indicated in Ref. [36].

The covariant kinetic Lagrangian of the Higgs boson triplets generates mass for nine gauge bosons  $\mathcal{L}^\phi = \sum_{\phi=\chi,\eta,\rho} (D_\mu \phi)^\dagger (D^\mu \phi)$ , where  $D_\mu = \partial_\mu - igW_\mu^a T^a - ig_X T^9 X X_\mu$ , with  $a = 1, 2, \dots, 8$ , and  $T^9 \equiv \frac{I_3}{\sqrt{6}}$  and  $\frac{1}{\sqrt{6}}$  corresponding to (anti)triplets and singlets [10]. The matrix  $W^a T^a$  can be presented as

$$W_\mu^a T^a = \frac{1}{2} \begin{pmatrix} W_\mu^3 + \frac{1}{\sqrt{3}}W_\mu^8 & \sqrt{2}W_\mu^+ & 0 \\ \sqrt{2}W_\mu^- & -W_\mu^3 + \frac{1}{\sqrt{3}}W_\mu^8 & \sqrt{2}Y_\mu^+ \\ 0 & \sqrt{2}Y_\mu^- & -\frac{2}{\sqrt{3}}W_\mu^8 \end{pmatrix}, \quad (1)$$

where  $T^a = \lambda_a/2$  is respective to a triplet representation. The model consists of  $W^\pm$  and  $Y^\pm$ , which are two pairs of singly charged gauge bosons, as follows

$$W_\mu^\pm = \frac{1}{\sqrt{2}}(W_\mu^1 \mp iW_\mu^2), \quad Y_\mu^\pm = \frac{1}{\sqrt{2}}(W_\mu^6 \pm iW_\mu^7), \quad (2)$$

with the respective masses  $m_W^2 = \frac{g^2}{4}(v_1^2 + v_2^2)$  and  $m_Y^2 = \frac{g^2}{4}(w^2 + v_1^2)$ . The model will be

broken step by step as  $SU(3)_L \times U(1)_X \xrightarrow{w} SU(2)_L \times U(1)_Y \xrightarrow{v_1, v_2} U(1)_Q$ , where the vevs satisfy the hierarchy  $w \gg v_1, v_2$ . This leads to identifying  $W^\pm$  as the SM ones. Therefore the following relations are obtained as follows [36]

$$v_2^2 + v_1^2 \equiv v^2 = (246\text{GeV})^2, \quad \frac{g_X}{g} = \frac{3\sqrt{2}s_W}{\sqrt{3-4s_W^2}}, \quad s_W = \frac{e}{g}, \quad (3)$$

where  $e$  and  $s_W$  are the electric charge and sine of the Weinberg angle  $s_W^2 \simeq 0.231$  [37], respectively. Similarly to the 2HDM, the following parameters will be used

$$t_\beta \equiv \tan \beta = \frac{v_2}{v_1}, \quad v_1 = c_\beta \times v, \quad v_2 = s_\beta \times v. \quad (4)$$

The lepton masses generated from the Yukawa Lagrangian are below

$$\mathcal{L}_l^Y = -h_{ab}^e \overline{L}_a \rho e_{bR} + h_{ab}^\nu \epsilon^{ijk} \overline{(L_a)_i} (L_b)_j \rho_k^* - y_{ba}^X \overline{X_{bR}} \chi^\dagger L_a - \frac{1}{2} (\mu_X)_{ab} \overline{X_{aR}} (X_{bR})^c + \text{h.c.}, \quad (5)$$

where  $a, b = 1, 2, 3$ . The charged lepton masses generated from the first term of Eq. (5) as  $m_{e_a} \equiv \frac{h_{ab}^e v_1}{\sqrt{2}} \delta_{ab}$ , where we assume that the flavor states are physical. The 331NL model under consideration inherits lepton sector and LFV couplings given in Eq. (5), which are completely different from the class of the 3-3-1 models with six neutral lepton singlets mentioned in Ref. [1]. Namely, the 331NL consists of three exotic neutrinos in the  $SU(3)_L$  lepton triplets. Three other  $SU(3)_L$  singlets of neutral leptons are needed to work the ISS mechanism.

In the basis  $n'_L = (\nu_L, N_L, (X_R)^c)^T$ , Eq. (5) gives a neutrino mass term with the total  $9 \times 9$  mass matrix written in terms of the following block form of  $3 \times 3$  sub-matrices [38]

$$-\mathcal{L}_{\text{mass}}^\nu = \frac{1}{2} \overline{(n'_L)^c} \mathcal{M}^\nu n'_L + \text{h.c.}, \quad \text{where} \quad \mathcal{M}^\nu = \begin{pmatrix} \mathcal{O}_3 & m_D^T & \mathcal{O}_3 \\ m_D & \mathcal{O}_3 & M_R^T \\ \mathcal{O}_3 & M_R & \mu_X \end{pmatrix}, \quad (6)$$

where  $(n'_L)^c = ((\nu_L)^c, (N_L)^c, X_R)^T$ ,  $(M_R)_{ab} \equiv y_{ab}^X \frac{w}{\sqrt{2}}$ , and  $(m_D^T)_{ab} = -(m_D)_{ab} \equiv \sqrt{2} v_1 h_{ab}^\nu$  with  $a, b = 1, 2, 3$ . The matrix  $\mu_X$  in Eq. (5) is symmetric, so we consider it a diagonal one, simplifying the calculations without loss of generality.

By using the  $9 \times 9$  unitary matrix  $U^\nu$  that can diagonalize mass matrix  $\mathcal{M}^\nu$  as follows

$$U^{\nu T} \mathcal{M}^\nu U^\nu = \hat{M}^\nu = \text{diag}(m_{n_1}, m_{n_2}, \dots, m_{n_9}) = \text{diag}(\hat{m}_\nu, \hat{M}_N), \quad (7)$$

where the physical states  $n_{iL}$  have masses corresponding to  $m_{n_i}$  ( $i = 1, 2, \dots, 9$ ). The two mass matrices  $\hat{m}_\nu = \text{diag}(m_{n_1}, m_{n_2}, m_{n_3})$  and  $\hat{M}_N = \text{diag}(m_{n_4}, m_{n_5}, \dots, m_{n_9})$ , correspond to the active extra neutrinos  $n_{aL}$  ( $a = 1, 2, 3$ ) and  $n_{iL}$  ( $I = 1, 2, \dots, 6$ ), respectively. The following approximate solution for the neutrino mixing matrix  $U^\nu$  is reasonable for any particular seesaw mechanisms:

$$U^\nu = \Omega \begin{pmatrix} U_{\text{PMNS}} & \mathcal{O}_{3 \times 6} \\ \mathcal{O}_{6 \times 3} & V \end{pmatrix}, \quad \Omega \simeq \begin{pmatrix} I_3 - \frac{1}{2}RR^\dagger & R \\ -R^\dagger & I_6 - \frac{1}{2}R^\dagger R \end{pmatrix}, \quad (8)$$

where  $U_{\text{PMNS}}$  is the Pontecorvo-Maki-Nagakawa-Sakata (PMNS) matrix, and  $R, V$  are  $3 \times 6$ ,  $3 \times 6$  matrices, respectively. To derive the ISS relations perturbatively, it is assumed that all entries of the matrix  $R$  satisfy  $|R_{aI}| \ll 1$ .

The flavor and mass eigenstates are shown through the following relation:

$$n'_L = U^\nu n_L, \quad \text{and } (n'_L)^c = U^{\nu*} (n_L)^c \equiv U^{\nu*} n_R, \quad (9)$$

where  $n_L \equiv (n_{1L}, n_{2L}, \dots, n_{9L})^T$ , and  $n_i$  represents the Majorana states with components  $(n_{iL}, n_{iR})^T$ .

We summarize here the ISS expressions:

$$R_2^* = m_D^T M_R^{-1}, \quad R_1^* = -R_2^* \mu_X (M_R^T)^{-1} \simeq \mathcal{O}_3, \quad (10)$$

$$m_\nu = R_2^* \mu_X R_2^\dagger = U_{\text{PMNS}}^* \hat{m}_\nu U_{\text{PMNS}}^\dagger = m_D^T M_R^{-1} \mu_X (M_R^{-1})^T m_D, \quad (11)$$

$$V^* \hat{M}_N V^\dagger = M_N + \frac{1}{2} M_N R^\dagger R + \frac{1}{2} R^T R^* M_N. \quad (12)$$

All independent parameters  $x_{12,13}$  and three entries of  $M^{-1} \equiv M_R^{-1} \mu_X (M_R^{-1})^T$  can be determined from experimental data of  $m_\nu$  [2, 38]. In particular the Dirac mass matrix exhibits an antisymmetric structure, given by

$$m_D = z e^{i\alpha_{23}} \times \tilde{m}_D, \quad \text{where } \tilde{m}_D = \begin{pmatrix} 0 & x_{12} & x_{13} \\ -x_{12} & 0 & 1 \\ -x_{13} & -1 & 0 \end{pmatrix}, \quad (13)$$

where  $\alpha_{23} \equiv \arg[h_{32}^\nu]$  and

$$z = \sqrt{2}|h_{32}^\nu|v_1 = \sqrt{2}|h_{23}^\nu|v_1 \equiv c_\beta z_0 \quad (14)$$

is a real and positive parameter. We note that  $z_0 = \sqrt{2}v|h_{23}^\nu|$  is considered as the scale of the Dirac mass matrix  $m_D$ . The perturbative limit of the Yukawa coupling  $h_{23}^\nu$  leads to an

upper constraint that  $z_0 < 1223$  GeV [38]. The phase  $\alpha_{23} = 0$  is chosen after redefining the phase of  $L_a$  in the second term of Eq. (5). The Eq. (11) gives  $(m_\nu)_{ij} = [m_D^T M^{-1} m_D]_{ij}$  for all  $i, j = 1, 2, 3$ , resulting in six independent functions. By inserting  $(m_\nu)_{ij}$  into the three remaining relations with  $i = j$ , we obtain

$$x_{12} = \frac{(m_\nu)_{12} (m_\nu)_{13} - (m_\nu)_{11} (m_\nu)_{23}}{(m_\nu)_{13} (m_\nu)_{23} - (m_\nu)_{12} (m_\nu)_{33}}, \quad x_{13} = \frac{(m_\nu)_{13}^2 - (m_\nu)_{11} (m_\nu)_{33}}{(m_\nu)_{13} (m_\nu)_{23} - (m_\nu)_{12} (m_\nu)_{33}}, \quad (15)$$

and  $\text{Det}[m_\nu] = 0$ . We express all parameter of the matrix  $\mu_X$  as certain but lengthy functions of  $(ze^{i\alpha_{32}})$ , all entries of  $M_R$  and  $m_\nu$  by using  $M^{-1} = M_R^{-1} \mu_X (M_R^{-1})^T$ . While experiment data help determine  $m_\nu$ , others are free parameters.

We consider in the limit that  $|R_2| \ll 1$ , based on Eq. (12), we can approximately determine the heavy neutrino masses, namely

$$V^* \hat{M}_N V^\dagger \simeq M_N. \quad (16)$$

For convenience, we identify the reduced matrix:

$$M_R \equiv ze^{i\alpha_{23}} \tilde{M}_R, \quad (\tilde{M}_R)_{ij} \equiv k_{ij}, \quad (17)$$

so that  $R_2^* = -\tilde{m}_D / \tilde{M}_R$ . Since the matrix  $M_R$  is always diagonalized by two unitary transformations  $V_L$  and  $V_R$  [39],

$$V_L^T M_R V_R = z \times \hat{k} = z \times \text{diag}(\hat{k}_1, \hat{k}_2, \hat{k}_3), \quad (18)$$

where all  $\hat{k}_{1,2,3}$  are always positive and  $\hat{k}_a \gg 1$ , so that all ISS relations are valid. Therefore,  $M_R$  is determined in terms of free parameters included in  $\hat{k}$ ,  $V_{L,R}$ . Based on Eq. (12), we can prove that the matrix  $V$  can be determined approximately as follows

$$V = \frac{1}{\sqrt{2}} \begin{pmatrix} V_R & iV_R \\ V_L & -iV_L \end{pmatrix} \rightarrow V^T M_N V = z \times \begin{pmatrix} \hat{k} & \mathcal{O}_{3 \times 3} \\ \mathcal{O}_{3 \times 3} & \hat{k} \end{pmatrix}. \quad (19)$$

Consequently, for any qualitative estimations, by using the crude approximations that heavy neutrino masses are  $m_{n_{a+3}} = m_{n_{a+6}} \simeq z \hat{k}_a$  with  $a=1,2,3$ ;  $R_1 \simeq \mathcal{O}_3$ ; and

$$U^\nu \simeq \begin{pmatrix} \left( I_3 - \frac{1}{2} R_2 R_2^\dagger \right) U_{\text{PMNS}} & \frac{1}{\sqrt{2}} R_2 V_L & \frac{-i}{\sqrt{2}} R_2 V_L \\ \mathcal{O}_3 & \frac{V_R}{\sqrt{2}} & \frac{iV_R}{\sqrt{2}} \\ -R_2^\dagger U_{\text{PMNS}} & \left( I_3 - \frac{R_2^\dagger R_2}{2} \right) \frac{V_R}{\sqrt{2}} & \left( I_3 - \frac{R_2^\dagger R_2}{2} \right) \frac{-iV_R}{\sqrt{2}} \end{pmatrix}. \quad (20)$$

We have verified that the mentioned approximations yield numerical results consistent with the calculations discussed in Ref. [35]. Based on Eq. (15), the Dirac mass matrix  $\tilde{m}_D$  will be determined numerically through the active neutrino matrix  $m_\nu$  given in Eq. (11), using the input of  $3\sigma$  ranges of neutrino oscillation data. We investigate the parameter space by scanning the free parameters  $z_0$ ,  $\hat{k}_{1,2,3}$ , and  $V_R$  within reasonable ranges. Using these values, we construct the total neutrino mixing matrix  $U^\nu$  defined in Eq. (20). Because  $V_L$  satisfies:

$$R_2 V_L = \tilde{m}_D^\dagger V_R^* \hat{k}^{-1}, \quad R_2 R_2^\dagger = \tilde{m}_D^\dagger V_R \hat{k}^{-2} \tilde{m}_D, \quad (21)$$

which is explicitly independent of  $V_L$ , all processes discussed here are weakly affected by  $V_L$ . Therefore,  $V_L$  will be fixed at  $V_L = I_3$  for the remainder of this study.

The Yukawa Lagrangian generating quark masses was presented in Ref. [36]. In this work, it is important to emphasize that the perturbative limit  $h_{33}^u < \sqrt{4\pi}$ , leading to a lower bound for  $v_2$ :  $v_2 > \frac{\sqrt{2}m_t}{\sqrt{4\pi}}$ . By combining this relationship with Eqs. (3) and (4), the lower bound for  $t_\beta \geq 0.3$ . From the tau mass,  $m_\tau = h_{33}^3 \times v c_\beta \sqrt{2} \rightarrow h_{33}^3 = m_\tau \sqrt{2} / (v c_\beta) < \sqrt{4\pi}$ , we derive the upper bound for  $t_\beta$ , resulting in the rather weak upper bound  $t_\beta = \sqrt{1/c_\beta^2 - 1} \leq 346$ .

## B. Higgs bosons

In this work, the Higgs potential respects the new general lepton number introduced in Ref. [36], namely

$$V_{higgs} = \sum_{\phi} \left[ \mu_\phi^2 \phi^\dagger \phi + \lambda_\phi (\phi^\dagger \phi)^2 \right] + \lambda_{12} (\eta^\dagger \eta) (\rho^\dagger \rho) + \lambda_{13} (\eta^\dagger \eta) (\chi^\dagger \chi) + \lambda_{23} (\rho^\dagger \rho) (\chi^\dagger \chi) \\ + \tilde{\lambda}_{12} (\eta^\dagger \rho) (\rho^\dagger \eta) + \tilde{\lambda}_{13} (\eta^\dagger \chi) (\chi^\dagger \eta) + \tilde{\lambda}_{23} (\rho^\dagger \chi) (\chi^\dagger \rho) + \sqrt{2} f \omega (\epsilon_{ijk} \eta^i \rho^j \chi^k + \text{h.c.}), \quad (22)$$

where  $f$  is a dimensionless term,  $\phi = \eta, \rho, \chi$ . In previous research, the minimum conditions of the Higgs potential and the identification of the SM-like Higgs boson were thoroughly examined, as seen in references such as Refs. [40, 41]. Here, we summarize the essential results: The 331NL model includes two pairs of singly charged Higgs boson, denoted as  $h_1^\pm, h_2^\pm$ , along with two Goldstone bosons  $G_W^\pm, G_Y^\pm$  of the singly charged gauge bosons  $W^\pm$ , and  $Y^\pm$ , respectively. The mass terms are  $m_{h_1^\pm}^2 = \left( \frac{\tilde{\lambda}_{12} v^2}{2} + \frac{f w^2}{s_\beta c_\beta} \right)$ ,  $m_{h_2^\pm}^2 = (v^2 c_\beta^2 + w^2) \left( \frac{\tilde{\lambda}_{23}}{2} + f t_\beta \right)$ , and  $m_{G_W}^2 = m_{G_Y}^2 = 0$ . The original and mass eigenstates of the charged Higgs bosons are



described as in Ref. [40] as

$$\begin{pmatrix} \eta^\pm \\ \rho_1^\pm \end{pmatrix} = \begin{pmatrix} -s_\beta & c_\beta \\ c_\beta & s_\beta \end{pmatrix} \begin{pmatrix} G_W^\pm \\ h_1^\pm \end{pmatrix}, \quad \begin{pmatrix} \rho_2^\pm \\ \chi^\pm \end{pmatrix} = \begin{pmatrix} -s_{13} & c_{13} \\ c_{13} & s_{13} \end{pmatrix} \begin{pmatrix} G_Y^\pm \\ h_2^\pm \end{pmatrix}, \quad (23)$$

where  $t_{13} = v_1/w$ , and

$$f = \frac{c_\beta s_\beta (2m_{h_1^\pm}^2 - \tilde{\lambda}_{12}v^2)}{2\omega^2}. \quad (24)$$

Three neutral gauge bosons are predicted by this model, where there is one zero eigenvalue corresponding to the massless photon. Defining [10]

$$s_{331} \equiv \sin \theta_{331} = \sqrt{1 - \frac{t_W^2}{3}}, \quad c_{331} \equiv \cos \theta_{331} = -\frac{t_W}{\sqrt{3}}, \quad (25)$$

The original and physical basis of the neutral gauge bosons are presented below

$$\begin{pmatrix} X_\mu \\ W_\mu^3 \\ W_\mu^8 \end{pmatrix} = \begin{pmatrix} s_{331} & 0 & c_{331} \\ 0 & 1 & 0 \\ c_{331} & 0 & -s_{331} \end{pmatrix} \begin{pmatrix} c_W & -s_W & 0 \\ s_W & c_W & 0 \\ 0 & 0 & 1 \end{pmatrix} \begin{pmatrix} 1 & 0 & 0 \\ 0 & c_\theta & -s_\theta \\ 0 & s_\theta & c_\theta \end{pmatrix} \begin{pmatrix} A_\mu \\ Z_{1\mu} \\ Z_{2\mu} \end{pmatrix} = C \begin{pmatrix} A_\mu \\ Z_{1\mu} \\ Z_{2\mu} \end{pmatrix}, \quad (26)$$

$$C = \begin{pmatrix} s_{331}c_W & (-s_{331}s_Wc_\theta + c_{331}s_\theta) & (s_{331}s_Ws_\theta + c_{331}c_\theta) \\ s_W & c_Wc_\theta & -s_\theta c_w \\ c_{331}c_W & -(c_{331}s_Wc_\theta + s_{331}s_\theta) & (c_{331}s_Ws_\theta - s_{331}c_\theta) \end{pmatrix}.$$

Next, the gauge bosons are defined such as  $Z_1 \equiv Z$  and  $Z_2 \equiv Z'$ , where  $Z$  is the boson found experimentally.

The model includes five CP - odd neutral scalar components contained in the five neutral Higgs boson  $\eta_1^0 = (v_2 + R_1 + iI_1)/\sqrt{2}$ ,  $\rho^0 = (v_1 + R_2 + iI_2)/\sqrt{2}$ ,  $\chi_2^0 = (\omega + R_3 + iI_3)/\sqrt{2}$ ,  $\eta_2^0 = (R_4 + iI_4)/\sqrt{2}$ , and  $\chi_1^0 = (R_5 + iI_5)/\sqrt{2}$ . Which have three Goldstone bosons of the neutral gauge bosons as  $Z, Z'$ , and  $X^0$ . Others are physical states with masses

$$m_{a_1}^2 = (s_\beta^2 v^2 + \omega^2) \left( ft_\beta^{-1} + \frac{1}{2}\tilde{\lambda}_{13} \right), \quad m_{a_2}^2 = f \left( \frac{\omega^2}{c_\beta s_\beta} + c_\beta s_\beta v^2 \right). \quad (27)$$

Consequently, the condition  $f > 0$  is required for the term  $f$ .

Examining the CP-even scalars, in two bases  $(\eta_2^0, \chi_1^0)$  and  $(\eta_1^0, \rho_1^0, \chi_1^0)$ , there are corresponding  $2 \times 2$  and  $3 \times 3$  sub-matrices for the masses of these Higgs boson, detailed

$$M_{0,3}^2 = \begin{pmatrix} \frac{c_\beta f \omega^2}{s_\beta} + 2s_\beta^2 \lambda_1 v^2 & c_\beta s_\beta \lambda_{12} v^2 - \omega^2 f & \omega(s_\beta \lambda_{13} - c_\beta f) v \\ c_\beta s_\beta \lambda_{12} v^2 - \omega^2 f & \frac{s_\beta f \omega^2}{c_\beta} + 2v^2 c_\beta^2 \lambda_2 & v\omega(c_\beta \lambda_{23} - s_\beta f) \\ v\omega(s_\beta \lambda_{13} - c_\beta f) & v\omega(c_\beta \lambda_{23} - s_\beta f) & 2\lambda_3 \omega^2 + c_\beta s_\beta f v^2 \end{pmatrix},$$

$$M_{0,2}^2 = \begin{pmatrix} \frac{1}{2}\omega^2 \left( \tilde{\lambda}_{13} + \frac{2c_\beta f}{s_\beta} \right) & \frac{1}{2}v\omega(\tilde{\lambda}_{13}s_\beta + 2c_\beta f) \\ \frac{1}{2}v\omega(\tilde{\lambda}_{13}s_\beta + 2c_\beta f) & \frac{1}{2}v^2 s_\beta(\tilde{\lambda}_{13}s_\beta + 2c_\beta f) \end{pmatrix}. \quad (28)$$

The matrix  $M_{0,2}^2$  has one zero value, and  $m_{h_4}^2 = \left( \frac{f}{t_\beta} + \frac{\tilde{\lambda}_{13}}{2} \right) (s_\beta^2 v^2 + \omega^2)$ , consistent with the Goldstone boson of  $X^0$  and the Higgs boson  $h_4^0$  (heavy neutral boson) with mass at the  $SU(3)_L$  breaking scale. Furthermore, research also shows that  $\text{Det}[M_{0,3}^2]|_{v=0} = 0$ , but  $\text{Det}[M_{0,3}^2] \neq 0$ . This implies that the electroweak scale needs to have at least one Higgs boson mass, which can be associated with the SM-like Higgs boson. Namely, it can be demonstrated that

$$C_1^h M_{0,3}^2 C_1^{hT}|_{v=0} = \text{diag} \left( 0, 2\lambda_3 w^2, f w^2 / (s_\beta c_\beta) \right), \quad C_1^h = \begin{pmatrix} s_\beta & c_\beta & 0 \\ -c_\beta & s_\beta & 0 \\ 0 & 0 & 1 \end{pmatrix}, \quad (29)$$

and  $C_1^h M_{0,3}^2 C_1^{hT} \equiv M_{0,3}'^2$  satisfying

$$\begin{aligned} (M_{0,3}'^2)_{11} &= 2v^2 (c_\beta^4 \lambda_2 + c_\beta^2 \lambda_{12} s_\beta^2 + \lambda_1 s_\beta^4), \\ (M_{0,3}'^2)_{22} &= 2v^2 s_\beta^2 c_\beta^2 (\lambda_1 - \lambda_{12} + \lambda_2) + \frac{f\omega^2}{c_\beta s_\beta}, \\ (M_{0,3}'^2)_{33} &= f v^2 s_\beta c_\beta + 2\lambda_3 \omega^2, \\ (M_{0,3}'^2)_{12} &= (M_{0,3}'^2)_{21} = v^2 s_\beta c_\beta (s_\beta^2 (\lambda_{12} - 2\lambda_1) - c_\beta^2 (\lambda_{12} - 2\lambda_2)), \\ (M_{0,3}'^2)_{13} &= (M_{0,3}'^2)_{31} = v\omega (-2f s_\beta c_\beta + c_\beta^2 \lambda_{23} + \lambda_{13} s_\beta^2), \\ (M_{0,3}'^2)_{32} &= (M_{0,3}'^2)_{23} = v\omega (f c_\beta^2 - f s_\beta^2 + s_\beta c_\beta (\lambda_{23} - \lambda_{13})). \end{aligned} \quad (30)$$

As a result, by using unitary transformation  $C_2^h$  with  $(C_2^h)_{ij} \sim \mathcal{O}(v/w)$  ( $i \neq j$ ) so that  $C_2^h M_{0,3}'^2 C_2^{hT} = \text{diag} (m_{h_1^0}^2, m_{h_2^0}^2, m_{h_3^0}^2)$  and  $m_{h_1^0}^2 \sim \mathcal{O}(v^2)$  [38]. Hence  $h_1^0 \equiv h$  is determined with the SM-like Higgs boson found by experiment at the LHC. Contributions to  $h_1^0$  come only from  $\text{Re}[\eta_1^0] = R_1/\sqrt{2}$  and  $\text{Re}[\rho_1^0] \sim / \sqrt{2}$ , in particular

$$R_1 = s_\beta \times h_1^0 - c_\beta \times h_2^0, \quad R_2 = c_\beta \times h_1^0 + s_\beta \times h_2^0. \quad (31)$$

Based on the presented result, the couplings and their one-loop contributions to the aforementioned decays will be derived and are shown in detail in the next section.

### III. COUPLINGS AND ANALYTIC FORMULAS

The effective amplitude for the decays  $Z(q) \rightarrow e_a^\pm(p_1)e_b^\mp(p_2)$  is given by [29, 42]

$$i\mathcal{M}(Z \rightarrow e_b^+ e_a^-) = \frac{ie}{16\pi^2} \bar{u}_a [\not{\epsilon} (\bar{a}_l P_L + \bar{a}_r P_R) + (p_1 \cdot \epsilon) (\bar{b}_l P_L + \bar{b}_r P_R)] v_b, \quad (32)$$

where  $\epsilon_\alpha(q)$ ,  $u_a(p_1)$ , and  $v_b(p_2)$  are the polarization of  $Z$  and two Dirac spinors, respectively. The massive gauge boson  $Z$  has three physical polarization states satisfying  $q \cdot \epsilon = 0$ , which implies that  $p_2 \cdot \epsilon = -p_1 \cdot \epsilon$  with  $q = p_1 + p_2$ . Therefore, Eq. (32) reduces to two dependent one-loop form factors proportional to  $p_2 \cdot \epsilon$  introduced in Ref. [29]. The correlating partial decay width is

$$\Gamma(Z \rightarrow e_b^+ e_a^-) = \frac{\sqrt{\lambda}}{16\pi m_Z^3} \times \left( \frac{e}{16\pi^2} \right)^2 \left( \frac{\lambda M_0}{12m_Z^2} + M_1 + \frac{\lambda M_2}{3m_Z^2} \right), \quad (33)$$

where  $\lambda = m_Z^4 + m_b^4 + m_a^4 - 2(m_Z^2 m_a^2 + m_Z^2 m_b^2 + m_a^2 m_b^2) \simeq m_Z^4$  because of  $m_a^2, m_b^2 \ll m_Z^2$ , and

$$\begin{aligned} M_0 &= (m_Z^2 - m_a^2 - m_b^2) (|\bar{b}_l|^2 + |\bar{b}_r|^2) - 4m_a m_b \text{Re} [\bar{b}_l \bar{b}_r^*] \\ &\quad - 4m_b \text{Re} [\bar{a}_r^* \bar{b}_l^* + \bar{a}_l^* \bar{b}_r^*] - 4m_a \text{Re} [\bar{a}_l^* \bar{b}_l^* + \bar{a}_r^* \bar{b}_r^*], \\ M_1 &= 4m_a m_b \text{Re} [\bar{a}_l \bar{a}_r^*], \\ M_2 &= \left[ 2m_Z^4 - m_Z^2 (m_a^2 + m_b^2) - (m_a^2 - m_b^2)^2 \right] (|\bar{a}_l|^2 + |\bar{a}_r|^2). \end{aligned} \quad (34)$$

The relevant one-loop diagrams contributing to the decay amplitude  $Z \rightarrow e_a e_b$  in the unitary gauge are illustrated in Fig. 1. The couplings of charged gauge bosons giving one-loop

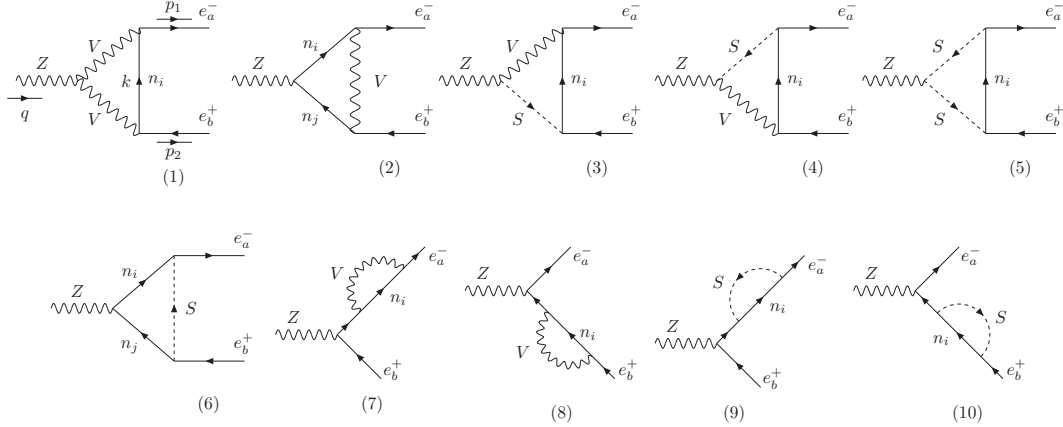


FIG. 1: One-loop Feynman diagrams contributing to  $Z \rightarrow e_a e_b$  in the unitary gauge [29]

contributions to LFVZ amplitudes are

$$\mathcal{L}_{\text{Vff}}^Y = \frac{g}{\sqrt{2}} \sum_{a=1}^3 \sum_{i=1}^9 \bar{n}_i \gamma^\mu P_L e_a [U_{ai}^{\nu*} W_\mu^+ + U_{(a+3)i}^{\nu*} Y_\mu^+] + h.c., \quad (35)$$

The couplings between gauge boson and two different leptons from Lagrangian in Eq. (35) are presented in Table II.

Vertex	Coupling
$W_\mu^+ \bar{n}_i e_b, W_\mu^- \bar{e}_a n_i,$	$\frac{ig}{\sqrt{2}} U_{ai}^{\nu*} \gamma^\mu P_L, \frac{ig}{\sqrt{2}} U_{ai}^\nu \gamma^\mu P_L$
$Y_\mu^+ \bar{n}_i e_b, Y_\mu^- \bar{e}_a n_i$	$\frac{ig}{\sqrt{2}} U_{(a+3)i}^{\nu*} \gamma^\mu P_L, \frac{ig}{\sqrt{2}} U_{(a+3)i}^\nu \gamma^\mu P_L$

TABLE II: Feynman rules relevant one-loop contributions to  $Z \rightarrow e_a e_b$  in the unitary gauge relate between gauge boson and two different leptons.

The couplings between three gauge bosons originate from the covariant kinetic Lagrangian of the non-Abelian gauge bosons:

$$\mathcal{L}_D^g = -\frac{1}{4} \sum_{a=1}^8 F_{\mu\nu}^a F^{a\mu\nu}, \quad (36)$$

where

$$F_{\mu\nu}^a = \partial_\mu W_\nu^a - \partial_\nu W_\mu^a + g \sum_{b,c=1}^8 f^{abc} W_\mu^b W_\nu^c, \quad (37)$$

where  $f^{abc}$  ( $a, b, c = 1, 2, \dots, 8$ ) are structure constants of the  $SU(3)$  group, which identified as

$$\begin{aligned} \mathcal{L}_D^g = & - \sum_{V=W,Y} eg_{ZVV} Z^\mu(p_0) V^{+\nu}(p_+) V^{-\lambda}(p_-) \times \Gamma_{\mu\nu\lambda}(p_0, p_+, p_-), \\ & - e \sum_{V=W,Y} A^\mu(p_0) V^{+\nu}(p_+) V^{-\lambda}(p_-) \times \Gamma_{\mu\nu\lambda}(p_0, p_+, p_-) + \dots, \end{aligned} \quad (38)$$

where  $\Gamma_{\alpha\beta\sigma}(p_0, p_+, p_-) \equiv g_{\alpha\beta}(p_0 - p_+)_\sigma + g_{\beta\sigma}(p_+ - p_-)_\alpha + g_{\sigma\alpha}(p_- - p_0)_\beta$ , and  $V = W^\pm, Y^\pm$ .

In Table III show the involving couplings of  $Z$ .

Vertex	Coupling
$g_{ZW+W^-}$	$t_W^{-1} c_\theta$
$g_{ZY+Y^-}$	$\frac{1}{2s_W} \left[ c_\theta c_W (1 - t_W^2) + s_\theta \sqrt{3 - t_W^2} \right]$

TABLE III: Feynman rules for triple gauge couplings corresponding with LFVZ decays.

The covariant kinetic terms of the Higgs bosons, which include the couplings of Higgs and gauge bosons, are presented as follows

$$\mathcal{L}_{\text{kin}}^\phi = \sum_{\phi=\chi,\rho,\eta} (D_\mu \phi)^\dagger (D^\mu \phi)$$

$$\begin{aligned}
&= g_{hWW}g_{\mu\nu}hW^{-\mu}W^{+\nu} + g_{hYY}g_{\mu\nu}hY^{-\mu}Y^{+\nu} \\
&+ \left[ -ig_{hh_1^\pm W}^* (h_1^+ \partial_\mu h - h \partial_\mu h_1^+) W^{-\mu} + ig_{h_1^\pm W} (h_1^- \partial_\mu h - h \partial_\mu h_1^-) W^{+\mu} \right] \\
&+ \left[ -ig_{hh_2^\pm Y}^* (h_2^+ \partial_\mu h - h \partial_\mu h_2^+) Y^{-\mu} + ig_{h_2^\pm Y} (h_2^- \partial_\mu h - h \partial_\mu h_2^-) Y^{+\mu} \right] \\
&+ \sum_{k=1}^2 ieA^\mu (h_k^- \partial_\mu h_k^+ - h_k^+ \partial_\mu h_k^-) + \sum_{k=1}^2 ieg_{Zh_k^+ h_k^-} Z^\mu (h_k^- \partial_\mu h_k^+ - h_k^+ \partial_\mu h_k^-) \\
&+ Z^\mu e \left[ ig_{ZW+h_1^-} W^{+\nu} h_1^- g_{\mu\nu} + ig_{ZW+h_1^-}^* W^{-\nu} h_1^+ g_{\mu\nu} \right] \\
&+ Z^\mu e \left[ ig_{ZY+h_2^-} Y^{+\nu} h_2^- g_{\mu\nu} + ig_{ZY+h_2^-}^* Y^{-\nu} h_2^+ g_{\mu\nu} \right] + \text{irrelevant terms.} \quad (39)
\end{aligned}$$

Next, we present the corresponding terms contributing to the decays  $Z \rightarrow e_a e_b$  from the second line in Eq. (39). Table IV shows the relevant Feynman rules, where  $\partial_\mu h \rightarrow -ip_{0\mu} h$  and  $\partial_\mu h_i^\pm \rightarrow -ip_{\pm\mu} h_i^\pm$ , leading to  $i(h_i^- \partial_\mu h_i^+ - h_i^+ \partial_\mu h_i^-) = h_i^- h_i^+ (p_+ - p_-)_\mu$ . The incoming momenta are denoted  $p_0, p_\pm$ .

Vertex	Coupling	
$g_{Zh_1^+ h_1^-}$	$\frac{1}{2c_W s_W}$	$c_\theta (1 - 2s_W^2) + \frac{c_W s_\theta (2\sqrt{3}c_\beta^2 - \frac{1}{\sqrt{3}}t_W^2 - \sqrt{3})}{3\sqrt{1 - \frac{1}{3}t_W^2}}$
$g_{Zh_2^+ h_2^-}$	$\frac{1}{2s_W c_W}$	$c_\theta (s_{13}^2 - 2s_W^2) - \frac{s_\theta (c_{13}^2 - 2)(2s_W^2 - 1)}{\sqrt{3 - 4s_W^2}}$
$g_{ZW+h_1^-}$	$-\frac{s_\theta s_{2\beta} m_W}{t_W \sqrt{3 - 4s_W^2}}$	
$g_{ZY+h_2^-}$	$-\frac{c_\beta c_{13} m_W}{c_W s_W}$	$c_\theta + \frac{s_\theta (-1 + 2s_W^2)}{\sqrt{3 - 4s_W^2}}$

TABLE IV: Feynman rules of couplings with  $Z$  to charged Higgs and gauge bosons.

The Lagrangian with  $Z$  couplings to leptons is given by:

$$\begin{aligned}
L_{Z\ell\ell} &= e \left( c_\theta + \frac{s_\theta}{\sqrt{3 - 4s_W^2}} \right) \bar{e}_a \gamma^\mu \left[ \frac{1}{s_W c_W} \left( -\frac{1}{2} + s_W^2 \right) P_L + t_W P_R \right] e_a Z_{1\mu} \\
&+ \frac{ec_\theta}{2c_W s_W} \left[ \left( 1 + \frac{t_\theta (2s_W^2 - 1)}{\sqrt{3 - 4s_W^2}} \right) \bar{\nu}_a \gamma^\mu P_L \nu_a + \frac{4t_\theta c_W^2}{\sqrt{3 - 4s_W^2}} \bar{N}_a \gamma^\mu P_L N_a \right] Z_{1\mu}. \quad (40)
\end{aligned}$$

Returning according to Feynman rules, the couplings of the  $Z$  to two Majorana leptons  $n_i$  and  $n_j$  can be expressed using the form:

$$\begin{aligned}
\mathcal{L}_{Z\ell\ell} &= \sum_{i,j=1}^9 \left[ \frac{e}{2} \bar{n}_i \gamma^\mu (G_{ij} P_L - G_{ji} P_R) n_j Z_\mu \right], \\
G_{ij} &= \frac{c_\theta}{2c_W s_W} \sum_{c=1}^3 \left[ \left( 1 + \frac{t_\theta (2s_W^2 - 1)}{\sqrt{3 - 4s_W^2}} \right) U_{ci}^{\nu*} U_{cj}^\nu + \frac{4t_\theta c_W^2}{\sqrt{3 - 4s_W^2}} U_{(c+3)i}^{\nu*} U_{(c+3)j}^\nu \right]. \quad (41)
\end{aligned}$$

Therefore, we consider the limit  $\theta = 0$ , which leads to the same coupling of  $Z$  as given in Ref. [1], consistent with 2HDM results.

$$\mathcal{L}_{\text{int}} = \sum_{i,j=1}^9 \left[ -\frac{g}{4m_W} \bar{n}_i (\lambda_{ij}^h P_L + \lambda_{ij}^{h*} P_R) n_j h + \frac{e}{2} \bar{n}_i \gamma^\mu (G_{ij} P_L - G_{ji} P_R) n_j Z_\mu \right], \quad (42)$$

where

$$\lambda_{ij}^h = \lambda_{ji}^h = \sum_{c=1}^3 (U_{ci}^{\nu*} m_{n_i} U_{cj}^\nu + U_{cj}^{\nu*} m_{n_j} U_{ci}^\nu). \quad (43)$$

Following Ref. [11], the Yukawa couplings of leptons with charged Higgs boson are identified as

$$\mathcal{L}^{\ell n h^\pm} = -\frac{g}{\sqrt{2}m_W} \sum_{k=1}^2 \sum_{a=1}^3 \sum_{i=1}^9 h_k^+ \bar{n}_i (\lambda_{ai}^{L,k} P_L + \lambda_{ai}^{R,k} P_R) e_a + \text{h.c.}, \quad (44)$$

we defined

$$\begin{aligned} \lambda_{ai}^{R,1} &= m_a t_\beta U_{ai}^{\nu*}, & \lambda_{ai}^{L,1} &= s_\beta z_0 e^{i\alpha_{23}} \sum_{c=1}^3 (\tilde{m}_D)_{ac} U_{(c+3)i}^\nu, \\ \lambda_{ai}^{R,2} &= \frac{m_a c_\theta U_{(a+3)i}^{\nu*}}{c_\beta}, & \lambda_{ai}^{L,2} &= c_\theta z_0 \sum_{c=1}^3 \left[ -e^{i\alpha_{23}} (\tilde{m}_D)_{ac} U_{ci}^\nu + t_\theta^2 (\tilde{M}_R^T)_{ac} U_{(c+6)i}^\nu \right]. \end{aligned} \quad (45)$$

Additionally, one-loop contributions of the decays  $h \rightarrow e_a e_b$  were introduced previously, see Ref. [11], which will be used to investigate simultaneously with LFVZ and cLFV decays in this work. We will use the analytical formulas given in Ref. [11].

#### IV. NUMERICAL DISCUSSION

In this paper, we will use the neutrino oscillation data provided in Refs. [43, 44]. The lepton mixing matrix  $U_{\text{PMNS}}$  has the standard form as a function of parameters defined from the experimental data, namely the three mixing angles  $\theta_{ij}$  [43–45], one Dirac phase  $\delta$  and two Majorana phases  $\alpha_1$  and  $\alpha_2$  [45], in particular

$$\begin{aligned} U_{\text{PMNS}}^{\text{PDG}} &= f(\theta_{12}, \theta_{13}, \theta_{23}, \delta) \times \text{diag}(1, e^{i\alpha_1}, e^{i\alpha_2}), \\ f(\theta_{12}, \theta_{13}, \theta_{23}, \delta) &\equiv \begin{pmatrix} 1 & 0 & 0 \\ 0 & c_{23} & s_{23} \\ 0 & -s_{23} & c_{23} \end{pmatrix} \begin{pmatrix} c_{13} & 0 & s_{13} e^{-i\delta} \\ 0 & 1 & 0 \\ -s_{13} e^{i\delta} & 0 & c_{13} \end{pmatrix} \begin{pmatrix} c_{12} & s_{12} & 0 \\ -s_{12} & c_{12} & 0 \\ 0 & 0 & 1 \end{pmatrix}, \end{aligned} \quad (46)$$

where  $c_{ij} \equiv \cos \theta_{ij}$ ,  $s_{ij} \equiv \sin \theta_{ij}$ ,  $i, j = 1, 2, 3$  ( $i < j$ ),  $0 \leq \theta_{ij} < 90$  [Deg.] and  $0 < \delta \leq 720$  [Deg.]. We fix the range  $-180 \leq \alpha_i \leq 180$  [Deg.] for the Majorana phases. For numerical research, benchmark related to the NO (normal order) of the neutrino oscillation data [37] will be selected as the input to fix  $\tilde{m}_D$ . Specifically, these parameters are:  $s_{12}^2 = 0.32$ ,  $s_{13}^2 = 0.0216$ ,  $s_{23}^2 = 0.547$ ,  $\Delta m_{32}^2 = 2.424 \times 10^{-3}[\text{eV}^2]$ ,  $\Delta m_{21}^2 = 7.55 \times 10^{-5}[\text{eV}^2]$ ,  $\delta = 180$  [Deg], and  $\alpha_1 = \alpha_2 = 0$ . As a consequence, the matrix  $\tilde{m}_D$ , which the reduced Dirac mass matrix, is chosen below

$$\tilde{m}_D = \begin{pmatrix} 0 & 0.613 & 0.357 \\ -0.613 & 0 & 1 \\ -0.357 & -1 & 0 \end{pmatrix}. \quad (47)$$

The mixing matrix  $V_R$  is parameterized similarly as  $V_R = f(\theta_{12}^r, \theta_{13}^r, \theta_{23}^r, 0)$ , where the scanning ranges for the angles  $\theta_{ij}^r \in [0, 2\pi]$ . The remaining free terms are explored within the following ranges:

$$\begin{aligned} \hat{k}_{1,2,3} &\geq 5, \quad 1 \text{ [TeV]} \leq m_{h_1^\pm}, m_{h_2^\pm} \leq 5 \text{ [TeV]}, \\ t_\beta &\in [0.5, 40], \quad 100 \text{ [GeV]} \leq z \leq 600 \text{ [GeV]}. \end{aligned} \quad (48)$$

$G_F = 1.663787 \times 10^{-5} \text{ [GeV}^{-2}]$ ,  $\alpha_{em} = e^2/(4\pi) = 1/137$ ,  $g = 0.652$ ,  $s_W^2 = 0.231$ ,  $m_e = 5.0 \times 10^{-4} \text{ [GeV]}$ ,  $m_\mu = 0.105 \text{ [GeV]}$ ,  $m_\tau = 1.776 \text{ [GeV]}$ ,  $m_Z = 91.1876 \text{ [GeV]}$ , and  $m_W = 80.385 \text{ [GeV]}$ , and the total decay width of the  $Z$  boson is  $\Gamma_Z = 2.4955 \text{ [GeV]}$ . These parameters are found experimentally [37]. The well-known decays branching ratios used in this research are  $\text{Br}(\mu \rightarrow e \bar{\nu}_e \nu_\mu) \simeq 1$ ,  $\text{Br}(\tau \rightarrow \mu \bar{\nu}_\mu \nu_\tau) \simeq 0.1739$ , and  $\text{Br}(\tau \rightarrow e \bar{\nu}_e \nu_\tau) \simeq 0.1782$  [37]. The scanning ranges of  $\hat{k}_{1,2,3}$  are suggested based on the numerical checks in Refs. [35, 46], where the values of  $k_{ij}$  given in Eq. (17) must satisfy the ISS relation, i.e.,  $|k_{ij}| \simeq |M_R|/|m_D| \gg 1 \forall i, j = 1, 2, 3$ . Note that the values of  $k_{ij}$  relate to  $\hat{k}_{1,2,3}$  through Eq. (18).

In the numerical investigation, all collected points presented in the following figures satisfy current experimental constraints on the decay rates of cLFV, LFV $h$ , and LFV $Z$  decays. The dependence of the LFV decay rates on  $z_0$  is presented in Fig. 2. The upper bounds of cLFV decays are consistent with current experimental constraints, as shown in Refs. [13–16] and detailed in Table I. The future sensitivity of  $\text{Br}(\mu \rightarrow e\gamma)$ ,  $\text{Br}(\tau \rightarrow \mu\gamma)$ , and  $\text{Br}(\tau \rightarrow e\gamma)$  may reach orders of  $\mathcal{O}(10^{-14})$ ,  $\mathcal{O}(10^{-9})$ , and  $\mathcal{O}(10^{-9})$ , respectively, as shown in Table I [17, 18]. Therefore, the upper bounds on the branching ratios of these decays will be larger than the future sensitivity.

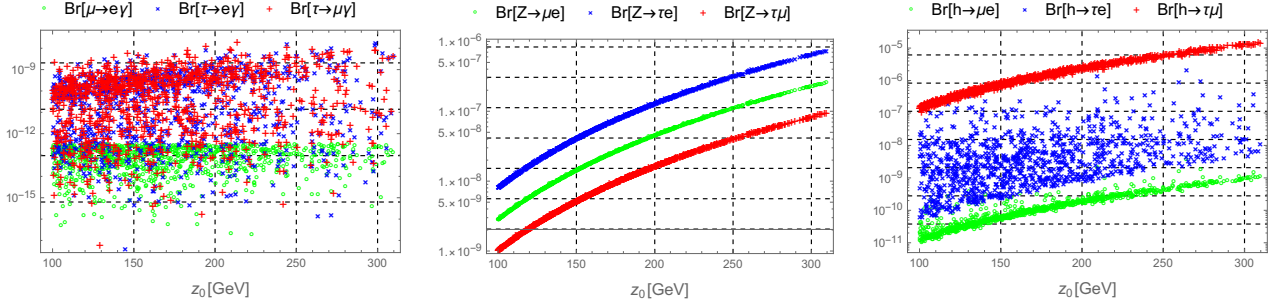


FIG. 2: The dependence of LFV decay rates on  $z_0$ .

According to illustrated in Fig. 2, we can see that LFVZ decay rates strongly depend on  $z_0$ , shown in three narrow curves in the middle panel of Fig. 2. Additionally, an interesting consequence in the 331NL model is that the upper constraint of  $\text{Br}(Z \rightarrow \mu^+ e^-) \leq 2.6 \times 10^{-7}$  is consistent with the experimental data in Table I. The two LFVh decays,  $h \rightarrow \mu e$  and  $h \rightarrow \tau \mu$ , have upper bounds of  $\text{Br}(h \rightarrow \mu e) < 5 \times 10^{-9}$  and  $\text{Br}(h \rightarrow \tau \mu) < 2 \times 10^{-5}$ , providing the strictest upper bound on  $z_0$ , namely  $z_0 \leq 310$  GeV. Therefore, if one of these decay rates is detected, the remaining values can be predicted precisely.

Similarly, the dependence of LFV decays on  $t_\beta$  is shown in Fig. 3. Corresponding to the

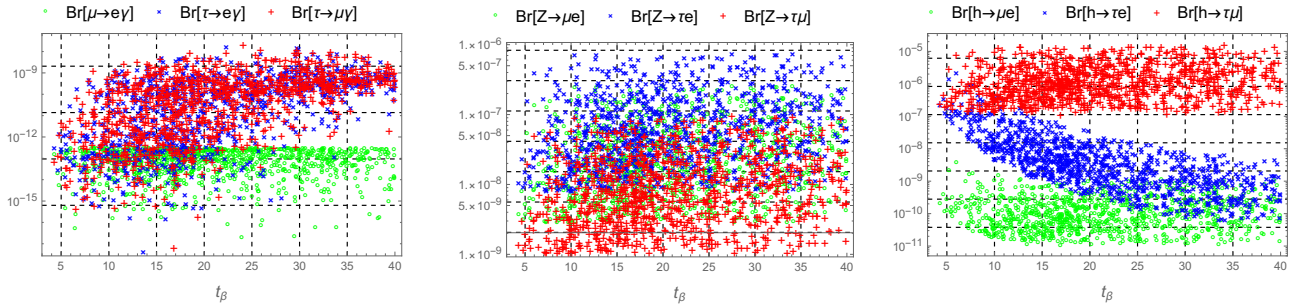


FIG. 3: The dependence of LFV decay rates on  $t_\beta$ .

chosen scanning range of the parameter  $t_\beta$  given in Eq. (48), we see that all  $\text{Br}(\text{LFV})$  depend on  $t_\beta$ , and the upper bounds are consistent with the constraints from current experiments as shown in Refs. [13–16]. However, the upper bounds on branching ratios in the left panel of Fig. 3 are larger than the future sensitivity, as demonstrated in the results in Fig. 2 [17, 18], see Table I. Next, the upper bound of LFVZ decays are  $\max[\text{Br}(Z \rightarrow \mu e)] \simeq 2.4 \times 10^{-7}$ ,  $\max[\text{Br}(Z \rightarrow \tau \mu)] \simeq 1. \times 10^{-7}$ , and  $\max[\text{Br}(Z \rightarrow \tau e)] \simeq 8.8 \times 10^{-7}$ . We can see that only the decay rate ( $Z \rightarrow \mu e$ ) is close to the latest experimental bound [24], with values of  $\mathcal{O}(10^{-7})$ . Besides that, the two other decays are still much smaller than the recent experimental



sensitivities as in Ref. [25], with values of  $\mathcal{O}(10^{-6})$ . However, the future sensitivities for these decays will be as at HL-LHC [26] and at FCC-ee [26, 27], see Table I. From these results, we can infer that although  $\text{Br}(Z \rightarrow \mu e)$  satisfied the recent experimental sensitivities, two other channels satisfied the future experimental data at HL-LHC [26]. However, all of them are still very difficult to detect at FCC-ee [26, 27]. In addition, the upper bounds of  $\text{Br}(h \rightarrow \mu e)$ ,  $\text{Br}(h \rightarrow \tau \mu)$  decays have the same result as in Fig. 2, and  $\text{Br}(h \rightarrow \tau e) < 5 \times 10^{-6}$ . The future experimental sensitivities at the HL-LHC and  $e^+e^-$  colliders may be of the order  $\mathcal{O}(10^{-5})$ ,  $\mathcal{O}(10^{-4})$ , and  $\mathcal{O}(10^{-4})$  [21–23] for the three mentioned previously LFVh decays, respectively. It is easily seen that only  $\text{Br}(h \rightarrow \tau \mu)$  is likely to reach a significant value within the near future experimental sensitivities at the HL-LHC and  $e^+e^-$  colliders.

The correlations between LFV decays and  $\text{Br}(\mu \rightarrow e\gamma)$  are illustrated in Fig. 4. We choose a survey value of  $\text{Br}(\mu \rightarrow e\gamma)$  that satisfies the experimental limits as in Ref. [13]. Satisfying the requirement of  $\text{Br}(e_b \rightarrow e_a\gamma)$  is the most stringent requirement in experiments. Therefore, all investigations of decay processes should satisfy this condition. The decay rate  $\text{Br}(\mu \rightarrow e\gamma)$  is the most stringently constrained by experiments. Future sensitivities of  $\mathcal{O}(10^{-9})$  continue to support all other decay rates reaching their respective expected sensitivities [28], especially with the upper bound of these decays being  $\text{Br}(\tau \rightarrow e(\mu)\gamma) \sim 10^{-8}$ . Our results show that all decay rates can reach the corresponding expected future sensitivities, except for  $\text{Br}(h \rightarrow \mu e)$ , which remains smaller than future experimental sensitivities.

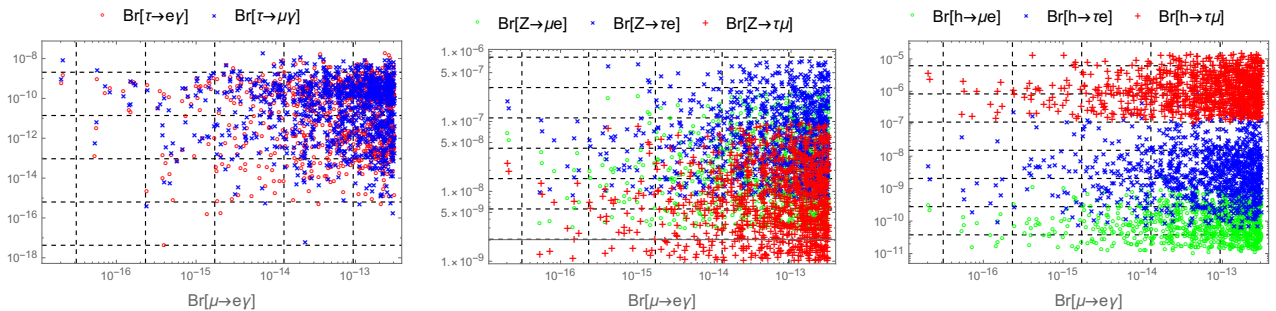


FIG. 4: The dependence of LFV decay rates on  $\text{Br}(\mu \rightarrow e\gamma)$ .

The correlations between LFVh and LFVZ decay rates are presented in Fig. 5. Over the value range of  $\text{Br}(h \rightarrow e_a e_b)$  that satisfies experimental constraints, all branching ratios of LFVZ decay channels strongly depend on these values, as shown in Fig. 5. Particularly, a large value of  $\text{Br}(h \rightarrow e_a e_b)$  predicts a correspondingly large value of  $\text{Br}(Z \rightarrow e_a e_b)$ . The

upper bounds of the branching ratios of these decay are close to the recent experimental data.

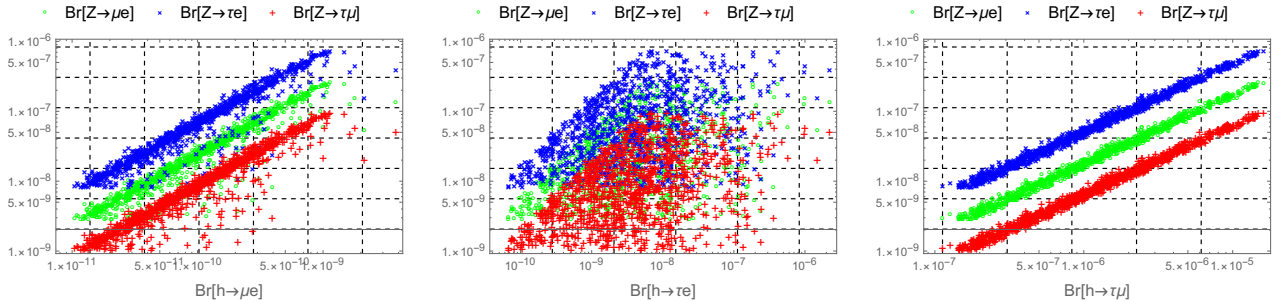


FIG. 5: The correlations between LFV $h$  and LFV $Z$  decay rates

## V. CONCLUSION

In the  $331NL$  model framework, we have studied the cLFV, LFV $h$ , and LFV $Z$  decays in detail and obtained many interesting results. Firstly, the numerical results showed a strong dependence of LFV $Z$  decay on  $z_0$ . In contrast, the dependencies of LFV decays on  $t_\beta$  are weaker. Only the decay rate ( $Z \rightarrow \mu e$ ) is close to the latest experimental bound, and  $\text{Br}(h \rightarrow \tau \mu)$  can reach the near future experimental sensitivities. Secondly,  $\text{Br}(\mu \rightarrow e \gamma)$  is significantly proportional to  $\text{Br}(Z \rightarrow \tau e)$  and  $\text{Br}(h \rightarrow \tau \mu)$ . All decay rates can reach the corresponding expected future sensitivities, except for  $\text{Br}(h \rightarrow \mu e)$ . Lastly,  $\text{Br}(h \rightarrow \mu e, \tau \mu)$  exhibit nearly linear correlation with  $\text{Br}(Z \rightarrow e_a e_b)$ . These clear dependencies indicate that if one of the two LFV $Z$  or LFV $h$  is observed by future experiments, the  $331NL$  model will predict the remaining decay rates. This model will also be confirmed or excluded if both LFV decay rates are measured experimentally. The upper bounds of  $\text{Br}(Z \rightarrow e_a e_b)$  also coincide with recent experiments and consistent with previous discussions [28]. In conclusion, the simultaneous study of the three LFV decay types in our work shows many interesting correlations that can be tested in upcoming experiments. Furthermore, the survey results are more reliable and our work helps narrow down the allowed regions of the parameter space that can be effectively probed by forthcoming experiments for LFV decays.

## Acknowledgments

This research is funded by An Giang University under grant number 23.01.CN.

## Appendix A: One-loop form factors for LFVZ decays the unitary gauge

The form factors are calculated in the unitary gauge as in Ref. [1] as below. Diagram (1) in Fig 1 give one-loop contributions:

$$\bar{a}_l^{nGG} = \sum_{i=1}^9 g_{ab}^{LL} g_{ZGG} \left\{ \left[ -4 + \frac{m_{n_i}^2}{m_G^2} \left( \frac{m_Z^2}{m_G^2} - 2 \right) \right] C_{00} + 2 (m_Z^2 - m_a^2 - m_b^2) X_3 \right. \\ \left. - \frac{1}{m_G^2} \left[ m_Z^2 (2m_{n_i}^2 C_0 + m_a^2 C_1 + m_b^2 C_2) \right. \right. \\ \left. \left. - m_{n_i}^2 (B_0^{(1)} + B_0^{(2)}) - m_a^2 B_1^{(1)} - m_b^2 B_1^{(2)} \right] \right\}, \quad (\text{A1})$$

$$\bar{a}_r^{nGG} = \sum_{i=1}^9 g_{ab}^{LL} g_{ZGG} m_a m_b \left[ \left( -4 + \frac{m_Z^2}{m_G^2} \right) X_3 + \frac{m_Z^2 - 2m_G^2}{m_G^4} C_{00} \right], \quad (\text{A2})$$

$$\bar{b}_l^{nGG} = \sum_{i=1}^9 g_{ab}^{LL} g_{ZGG} m_a \left[ 4 (X_3 - X_1) + \frac{m_Z^2 - 2m_G^2}{m_G^4} (m_{n_i}^2 X_{01} + m_b^2 X_2) - \frac{2m_Z^2}{m_G^2} C_2 \right], \quad (\text{A3})$$

$$\bar{b}_r^{nGG} = \sum_{i=1}^9 g_{ab}^{LL} g_{ZGG} m_b \left[ 4 (X_3 - X_2) + \frac{m_Z^2 - 2m_G^2}{m_G^4} (m_{n_i}^2 X_{02} + m_a^2 X_1) - \frac{2m_Z^2}{m_G^2} C_1 \right], \quad (\text{A4})$$

where  $g_{ab}^{LL} \equiv g_{aiG}^{L*} g_{biG}^L$ , the PV-functions  $B_{0,1}^{(k)} = B_{0,1}^{(k)}(p_k^2; m_{n_i}^2, m_G^2)$ ,  $C_{00,0,k,kl} = C_{00,0,k,kl}(m_a^2, m_Z^2, m_b^2; m_{n_i}^2, m_G^2, m_G^2)$ , and  $X_{0,k,kl}$  are identified in terms of the PV-functions for all  $k, l = 1, 2$ .

One-loop form factors from diagram (2) in Fig. 1 are:

$$\bar{a}_l^{Gnn} = \sum_{i,j=1}^9 \frac{g_{ab}^{LL}}{m_G^2} \left\{ G_{ij} \left[ m_G^2 \left( 4C_{00} + 2m_a^2 X_{01} + 2m_b^2 X_{02} - 2m_Z^2 (C_{12} + X_0) \right) \right. \right. \\ \left. \left. - (m_{n_i}^2 - m_a^2) B_0^{(1)} - (m_{n_j}^2 - m_b^2) B_0^{(2)} + m_a^2 B_1^{(1)} + m_b^2 B_1^{(2)} \right. \right. \\ \left. \left. + (m_{n_j}^2 m_a^2 + m_{n_i}^2 m_b^2 - m_a^2 m_b^2) X_0 - m_{n_i}^2 m_{n_j}^2 C_0 \right. \right. \\ \left. \left. - m_{n_i}^2 m_b^2 C_1 - m_{n_j}^2 m_a^2 C_2 \right] \right. \\ \left. + G_{ji} m_{n_i} m_{n_j} \left[ 2m_G^2 C_0 - 2C_{00} - m_a^2 C_{11} - m_b^2 C_{22} \right. \right. \\ \left. \left. + (m_Z^2 - m_a^2 - m_b^2) C_{12} \right] \right\}, \quad (\text{A5})$$

$$\bar{a}_r^{Gnn} = \sum_{i,j=1}^9 \frac{g_{ab}^{LL}}{m_G^2} m_a m_b G_{ij} \left[ 2C_{00} + 2m_G^2 X_0 + m_a^2 X_1 + m_b^2 X_2 - m_Z^2 C_{12} - m_{n_i}^2 C_1 - m_{n_j}^2 C_2 \right], \quad (\text{A6})$$

$$\bar{b}_l^{Gnn} = \sum_{i,j=1}^9 \frac{g_{ab}^{LL}}{m_G^2} m_a \left[ G_{ij} \left( -2m_G^2 X_{01} - m_b^2 X_2 + m_{n_j}^2 C_2 \right) + G_{ji} m_{n_i} m_{n_j} (X_1 - C_1) \right], \quad (\text{A7})$$

$$\bar{b}_r^{Gnn} = \sum_{i,j=1}^9 \frac{g_{ab}^{LL}}{m_G^2} m_b \left[ G_{ij} \left( -2m_G^2 X_{02} - m_a^2 X_1 + m_{n_i}^2 C_1 \right) + G_{ji} m_{n_i} m_{n_j} (X_2 - C_2) \right], \quad (\text{A8})$$

where  $g_{ab}^{LL} \equiv g_{aiG}^{L*} g_{bjG}^L$ ,

$$B_{0,1}^{(1)} = B_{0,1}^{(1)}(p_1^2; m_G^2, m_{n_i}^2), B_{0,1}^{(2)} = B_{0,1}^{(2)}(p_2^2; m_G^2, m_{n_j}^2),$$

and  $C_{00,0,k,kl} = C_{00,0,k,kl}(m_a^2, m_Z^2, m_b^2; m_G^2, m_{n_i}^2, m_{n_j}^2)$  for  $k, l = 1, 2$ .

Two diagrams (7) and (8) in Fig. 1 give sum contributions that have form factors

$$\bar{a}_l^{nG} = \frac{g_{Ze}^L}{m_G^2(m_a^2 - m_b^2)} \sum_{i=1}^9 g_{ab}^{LL} \left\{ 2m_{n_i}^2 (m_a^2 B_0^{(1)} - m_b^2 B_0^{(2)}) + m_a^4 B_1^{(1)} - m_b^4 B_1^{(2)} \right. \\ \left. + (2m_G^2 + m_{n_i}^2) (m_a^2 B_1^{(1)} - m_b^2 B_1^{(2)}) \right\}. \quad (\text{A9})$$

$$\bar{a}_r^{nG} = \frac{m_a m_b g_{Ze}^R}{m_G^2(m_a^2 - m_b^2)} \sum_{i=1}^9 g_{ab}^{LL} \left\{ 2m_{n_i}^2 (B_0^{(1)} - B_0^{(2)}) + m_a^2 B_1^{(1)} - m_b^2 B_1^{(2)} \right. \\ \left. + (2m_G^2 + m_{n_i}^2) (B_1^{(1)} - B_1^{(2)}) \right\}, \quad (\text{A10})$$

$$\bar{b}_l^{nG} = \bar{b}_r^{nG} = 0, \quad (\text{A11})$$

where  $g_{ab}^{XY} \equiv g_{aiG}^{X*} g_{biG}^Y$  with  $X, Y = L, R$ , and  $B_{0,1}^{(k)} = B_{0,1}^{(k)}(p_k^2; m_{n_i}^2, m_G^2)$  with  $k = 1, 2$ .

In the limit  $\theta = 0$ , the contributions from  $W^\pm$  corresponding to diagrams (1), (2), (7), and (8) of Fig. 1 are:

$$m_G = m_W, g_{ZGG} = g_{ZWW} = t_W^{-1}, g_{aiG}^L = g_{aiW}^L = \frac{g}{\sqrt{2}} U_{ai}^{\nu*}, \quad (\text{A12})$$

and  $G_{ij}$  is given in Eq. (41).

The contributions from  $Y^\pm$  corresponding to diagrams (1), (2), (7), and (8) of Fig. 1 are:

$$m_G = m_Y, g_{ZGG} = g_{ZYY} = \frac{1 - t_W^2}{t_W}, g_{aiG}^L = g_{aiY}^L = \frac{g}{\sqrt{2}} U_{(a+3)i}^{\nu*}, \quad (\text{A13})$$

The two diagrams (3) and (4) appearing in the model under consideration were not discussed previously, we list here for completeness the form factors of diagram (3) in Fig. 1

are:

$$\begin{aligned}
\bar{a}_l^{nGH} &= \sum_{i=1}^9 -\frac{g_{ZGH}g_{aiG}^{L*}}{m_G^2} [g_{biH}^L m_{n_i} (m_G^2 C_0 - C_{00}) - g_{biH}^R m_b m_G^2 C_2], \\
\bar{a}_r^{nGH} &= \sum_{i=1}^9 -\frac{g_{ZGH}g_{aiG}^{L*}}{m_G^2} \times g_{biH}^R m_a (C_{00} + m_G^2 C_1), \\
\bar{b}_l^{nGH} &= \sum_{i=1}^9 -\frac{g_{ZGH}g_{aiG}^{L*}}{m_G^2} [m_a (g_{biH}^R m_b X_2 - g_{biH}^L m_{n_i} X_{01})], \\
\bar{b}_r^{nGH} &= \sum_{i=1}^9 -\frac{g_{ZGH}g_{aiG}^{L*}}{m_G^2} [g_{biH}^R (m_{n_i}^2 X_0 + m_a^2 X_1 - 2m_G^2 C_1) - g_{biH}^L m_{n_i} m_b X_2]. \tag{A14}
\end{aligned}$$

The contributions of the two diagrams (3) and (4) are suppressed due to the tiny mixing in  $g_{ZW h_1}$  and the large  $m_G = m_Y \gg m_W$ .

The form factors relating to diagram (4) are:

$$\begin{aligned}
\bar{a}_l^{nHG} &= \sum_{i=1}^9 -\frac{g_{ZGH}g_{biG}^L}{m_G^2} [g_{aiH}^{L*} m_{n_i} (m_G^2 C_0 - C_{00}) - g_{aiH}^{R*} m_a m_G^2 C_1], \\
\bar{a}_r^{nHG} &= \sum_{i=1}^9 -\frac{g_{ZGH}g_{biG}^L}{m_G^2} [g_{aiH}^{R*} m_b (m_G^2 C_2 + C_{00})], \\
\bar{b}_l^{nHG} &= \sum_{i=1}^9 -\frac{g_{ZGH}g_{biG}^L}{m_G^2} [g_{aiH}^{R*} (m_{n_i}^2 X_0 + m_b^2 X_2 - 2m_G^2 C_2) - g_{aiH}^{L*} m_a m_{n_i} X_1], \\
\bar{b}_r^{nHG} &= \sum_{i=1}^9 -\frac{g_{ZGH}g_{biG}^L m_b}{m_G^2} [g_{aiH}^{R*} m_a X_1 - g_{aiH}^{L*} m_{n_i} X_{02}], \tag{A15}
\end{aligned}$$

In this model, there are two classes of contributions, namely:

$$m_G = m_W, \quad m_H = m_{h_1^\pm}, \quad g_{aiH}^L = -\frac{g\lambda_{ai}^{L,1}}{\sqrt{2}m_W}, \quad g_{ZGH} = g_{ZW+h_1^-} = -\frac{s_\theta s_{2\beta} m_W}{t_W \sqrt{3 - 4s_W^2}} \rightarrow 0, \tag{A16}$$

and

$$m_G = m_Y, \quad m_H = m_{h_2^\pm}, \quad g_{aiH}^L = -\frac{g\lambda_{ai}^{L,2}}{\sqrt{2}m_W}, \quad g_{ZGH} = g_{ZY+h_2^-} = -\frac{c_\beta c_{13} m_W}{c_W s_W}. \tag{A17}$$

The scalar exchanges, determined based on previous works [1, 28, 29], give one-loop contributions. Form factors corresponding to diagrams (5) are:

$$\begin{aligned}
\bar{a}_l^{nss} &= -\frac{g^2}{m_W^2} \sum_{k=1}^2 \sum_{i=1}^9 g_{Zh_k^+ h_k^-} \lambda_{ai}^{L,k*} \lambda_{bi}^{L,k} C_{00}, \\
\bar{a}_r^{nss} &= -\frac{g^2}{m_W^2} \sum_{k=1}^2 \sum_{i=1}^9 g_{Zh_k^+ h_k^-} \lambda_{ai}^{R,k*} \lambda_{bi}^{R,k} C_{00}, \tag{A18}
\end{aligned}$$

$$\bar{b}_l^{nss} = -\frac{g^2}{m_W^2} \sum_{k=1}^2 \sum_{i=1}^9 g_{Zh_k^+ h_k^-} \left[ m_a \lambda_{ai}^{L,k*} \lambda_{bi}^{L,k} X_1 + m_b \lambda_{ai}^{R,k*} \lambda_{bi}^{R,k} X_2 - m_{n_i} \lambda_{ai}^{R,k*} \lambda_{bi}^{L,k} X_0 \right],$$

$$\bar{b}_r^{nss} = -\frac{g^2}{m_W^2} \sum_{k=1}^2 \sum_{i=1}^9 g_{Zh_k^+ h_k^-} \left[ m_a \lambda_{ai}^{R,k*} \lambda_{bi}^{R,k} X_1 + m_b \lambda_{ai}^{L,k*} \lambda_{bi}^{L,k} X_2 - m_{n_i} \lambda_{ai}^{L,k*} \lambda_{bi}^{R,k} X_0 \right],$$

where  $g_{Zh_k^+ h_k^-}$  is given in Table IV, and  $\lambda_{ab}^{XY,k} \equiv \lambda_{ai}^{X,k*} \lambda_{bj}^{Y,k}$  with  $X, Y = L, R$ . The arguments for PV-functions are  $(m_{n_i}^2, m_{h_k^\pm}^2, m_{h_k^\pm}^2)$ .

The contributions from diagram (6) is

$$\begin{aligned} \bar{a}_l^{snn} &= -\frac{g^2}{2m_W^2} \sum_{k=1}^2 \sum_{i,j=1}^9 \left\{ G_{ij} \left[ \lambda_{ab}^{LL,k} m_{n_i} m_{n_j} C_0 + \lambda_{ab}^{RL,k} m_a m_{n_j} (C_0 + C_1) \right. \right. \\ &\quad \left. \left. + \lambda_{ab}^{LR,k} m_b m_{n_i} (C_0 + C_2) + \lambda_{ab}^{RR,k} m_a m_b X_0 \right] \right. \\ &\quad \left. - G_{ji} \left[ -\lambda_{ab}^{LL,k} (2C_{00} + m_a^2 X_1 + m_b^2 X_2 - m_Z^2 C_{12}) \right. \right. \\ &\quad \left. \left. - m_a m_{n_i} \lambda_{ab}^{RL,k} C_1 - m_b m_{n_j} \lambda_{ab}^{LR,k} C_2 \right] \right\} \\ \bar{a}_r^{snn} &= -\frac{g^2}{2m_W^2} \sum_{k=1}^2 \sum_{i,j=1}^9 \left\{ G_{ij} \left[ -\lambda_{ab}^{RR,k} (2C_{00} + m_a^2 X_1 + m_b^2 X_2 - m_Z^2 C_{12}) \right. \right. \\ &\quad \left. \left. - \lambda_{ab}^{LR,k} m_a m_{n_i} C_1 - \lambda_{ab}^{RL,k} m_b m_{n_j} C_2 \right] \right. \\ &\quad \left. - G_{ji} \left[ \lambda_{ab}^{RR,k} m_{n_i} m_{n_j} C_0 + \lambda_{ab}^{LR,k} m_a m_{n_j} (C_0 + C_1) \right. \right. \\ &\quad \left. \left. + \lambda_{ab}^{RL,k} m_b m_{n_i} (C_0 + C_2) + \lambda_{ab}^{LL,k} m_a m_b X_0 \right] \right\}, \\ \bar{b}_l^{snn} &= -\frac{g^2}{m_W^2} \sum_{k=1}^2 \sum_{i,j=1}^9 \left[ G_{ij} \left( \lambda_{ab}^{RL,k} m_{n_j} C_2 + \lambda_{ab}^{RR,k} m_b X_2 \right) - G_{ji} \left( \lambda_{ab}^{RL,k} m_{n_i} C_1 + \lambda_{ab}^{LL,k} m_a X_1 \right) \right], \\ \bar{b}_r^{snn} &= -\frac{g^2}{m_W^2} \sum_{k=1}^2 \sum_{i,j=1}^9 \left[ G_{ij} \left( \lambda_{ab}^{LR,k} m_{n_i} C_1 + \lambda_{ab}^{RR,k} m_a X_1 \right) - G_{ji} \left( \lambda_{ab}^{LR,k} m_{n_j} C_2 + \lambda_{ab}^{LL,k} m_b X_2 \right) \right], \end{aligned} \tag{A19}$$

where  $\lambda_{ab}^{XY,k} \equiv \lambda_{ai}^{X,k*} \lambda_{bj}^{Y,k}$  with  $X, Y = L, R$ . The PV-functions and their linear combinations are  $F = F(m_a^2, m_Z^2, m_b^2; m_{h_k^\pm}^2, m_{n_i}^2, m_{n_j}^2)$  for all  $F = C_{00,0,i,ij}, X_{0,i}$  with  $i, j = 1, 2$ .

Sum of two diagrams (9) and (10) gives the following non-zero contributions

$$\begin{aligned} \bar{a}_l^{ns} &= -\frac{g^2 g_{Ze}^L}{2m_W^2 (m_a^2 - m_b^2)} \sum_{k=1}^2 \sum_{i=1}^9 \left[ m_{n_i} \left( m_a \lambda_{ab}^{RL,k} + m_b \lambda_{ab}^{LR,k} \right) \left( B_0^{(1)} - B_0^{(2)} \right) \right. \\ &\quad \left. - m_a m_b \lambda_{ab}^{RR,k} \left( B_1^{(1)} - B_1^{(2)} \right) - \lambda_{ab}^{LL,k} \left( m_a^2 B_1^{(1)} - m_b^2 B_1^{(2)} \right) \right], \\ \bar{a}_r^{ns} &= -\frac{g^2 g_{Ze}^R}{2m_W^2 (m_a^2 - m_b^2)} \sum_{k=1}^2 \sum_{i=1}^9 \left[ m_{n_i} \left( m_a \lambda_{ab}^{LR,k} + m_b \lambda_{ab}^{RL,k} \right) \left( B_0^{(1)} - B_0^{(2)} \right) \right. \end{aligned}$$

$$-m_a m_b \lambda_{ab}^{LL,k} \left( B_1^{(1)} - B_1^{(2)} \right) - \lambda_{ab}^{RR,k} \left( m_a^2 B_1^{(1)} - m_b^2 B_1^{(2)} \right) \Big], \quad (\text{A20})$$

where  $\lambda_{ab}^{XY,k} = \lambda_{ai}^{X,k*} \lambda_{bi}^{Y,k}$  with  $X, Y = L, R$ . The PV-functions are  $B_{0,1}^{(l)} = B_{0,1}(p_l^2; m_{n_i}^2, m_{h_k^\pm}^2)$  with  $k, l = 1, 2$ . In the limit  $\theta = 0$ , we derived that

$$\begin{aligned} \text{div}[\bar{a}_l^{nh_1^+ h_1^+}] &= A(m_D m_D^\dagger)_{ba} \times (-t_L), \quad \text{div}[\bar{a}_l^{h_1^+ nn}] = 0, \quad \text{div}[\bar{a}_l^{nh_2^+}] = A(m_D m_D^\dagger)_{ba} \times (t_L), \\ \text{div}[\bar{a}_l^{nh_2^+ h_2^+}] &= A(m_D m_D^\dagger)_{ba} \times (-t_W), \quad \text{div}[\bar{a}_l^{h_1^+ nn}] = \frac{A(m_D m_D^\dagger)_{ba}}{2s_W c_W}, \quad \text{div}[\bar{a}_l^{nh_2^+}] = A(m_D m_D^\dagger)_{ba} (t_L), \end{aligned}$$

where  $t_L = \frac{s_W^2 - c_W^2}{2s_W c_W}$  satisfy the divergent cancellation for the total amplitudes of LFVZ decays.

- 
- [1] T. T. Hong, L. T. T. Phuong, T. P. Nguyen, N. H. T. Nha and L. T. Hue, Phys. Rev. D **110**, no.7, 075010 (2024) doi:10.1103/PhysRevD.110.075010 [arXiv:2404.05524 [hep-ph]].
- [2] S. M. Boucenna, J. W. F. Valle and A. Vicente, Phys. Rev. D **92** (2015) no.5, 053001 [arXiv:1502.07546 [hep-ph]].
- [3] M. Singer, J. W. F. Valle and J. Schechter, Phys. Rev. D **22**, 738 (1980) doi:10.1103/PhysRevD.22.738
- [4] V. Pleitez and M. D. Tonasse, Phys. Rev. D **48**, 2353-2355 (1993) doi:10.1103/PhysRevD.48.2353 [arXiv:hep-ph/9301232 [hep-ph]].
- [5] P. H. Frampton, Phys. Rev. Lett. **69**, 2889-2891 (1992) doi:10.1103/PhysRevLett.69.2889
- [6] M. Ozer, Phys. Rev. D **54**, 1143-1149 (1996) doi:10.1103/PhysRevD.54.1143
- [7] R. Foot, H. N. Long and T. A. Tran, Phys. Rev. D **50** (1994) no.1, R34-R38 [arXiv:hep-ph/9402243 [hep-ph]].
- [8] R. A. Diaz, R. Martinez and F. Ochoa, Phys. Rev. D **69** (2004), 095009 [arXiv:hep-ph/0309280 [hep-ph]].
- [9] R. A. Diaz, R. Martinez and F. Ochoa, Phys. Rev. D **72** (2005), 035018 [arXiv:hep-ph/0411263 [hep-ph]].
- [10] A. J. Buras, F. De Fazio, J. Girrbach and M. V. Carlucci, JHEP **02**, 023 (2013) doi:10.1007/JHEP02(2013)023 [arXiv:1211.1237 [hep-ph]].

- [11] T. T. Hong, N. H. T. Nha, T. P. Nguyen, L. T. T. Phuong and L. T. Hue, PTEP **2022**, no.9, 093B05 (2022) doi:10.1093/ptep/ptac109 [arXiv:2206.08028 [hep-ph]].
- [12] A. Abada, J. Kriewald, E. Pinsard, S. Rosauero-Alcaraz and A. M. Teixeira, Eur. Phys. J. C **83** (2023) no.6, 494 [arXiv:2207.10109 [hep-ph]].
- [13] A. M. Baldini *et al.* [MEG], Eur. Phys. J. C **76** (2016) no.8, 434 [arXiv:1605.05081 [hep-ex]].
- [14] A. Abdesselam *et al.* [Belle], JHEP **10** (2021), 19 [arXiv:2103.12994 [hep-ex]].
- [15] K. Afanaciev *et al.* [MEG II], Eur. Phys. J. C **84**, no.3, 216 (2024) doi:10.1140/epjc/s10052-024-12416-2 [arXiv:2310.12614 [hep-ex]].
- [16] B. Aubert *et al.* [BaBar], Phys. Rev. Lett. **104** (2010), 021802 [arXiv:0908.2381 [hep-ex]].
- [17] A. M. Baldini *et al.* [MEG II], Eur. Phys. J. C **78** (2018) no.5, 380 [arXiv:1801.04688 [physics.ins-det]].
- [18] E. Kou *et al.* [Belle-II], PTEP **2019** (2019) no.12, 123C01 [erratum: PTEP **2020** (2020) no.2, 029201] [arXiv:1808.10567 [hep-ex]].
- [19] G. Aad *et al.* [ATLAS], Phys. Lett. B **801**, 135148 (2020) doi:10.1016/j.physletb.2019.135148 [arXiv:1909.10235 [hep-ex]].
- [20] A. M. Sirunyan *et al.* [CMS], Phys. Rev. D **104** (2021) no.3, 032013 [arXiv:2105.03007 [hep-ex]].
- [21] Q. Qin, Q. Li, C. D. Lü, F. S. Yu and S. H. Zhou, Eur. Phys. J. C **78**, no.10, 835 (2018) doi:10.1140/epjc/s10052-018-6298-7 [arXiv:1711.07243 [hep-ph]].
- [22] R. K. Barman, P. S. B. Dev and A. Thapa, Phys. Rev. D **107**, no.7, 075018 (2023) doi:10.1103/PhysRevD.107.075018 [arXiv:2210.16287 [hep-ph]].
- [23] M. Aoki, S. Kanemura, M. Takeuchi and L. Zamakhsyari, Phys. Rev. D **107**, no.5, 055037 (2023) doi:10.1103/PhysRevD.107.055037 [arXiv:2302.08489 [hep-ph]].
- [24] G. Aad *et al.* [ATLAS], Phys. Rev. D **108** (2023), 032015 [arXiv:2204.10783 [hep-ex]].
- [25] G. Aad *et al.* [ATLAS], Phys. Rev. Lett. **127** (2022), 271801 [arXiv:2105.12491 [hep-ex]].
- [26] M. Dam, SciPost Phys. Proc. **1** (2019), 041 [arXiv:1811.09408 [hep-ex]].
- [27] A. Abada *et al.* [FCC], Eur. Phys. J. C **79**, no.6, 474 (2019) doi:10.1140/epjc/s10052-019-6904-3
- [28] T. T. Hong, Q. D. Tran, T. P. Nguyen, L. T. Hue and N. H. T. Nha, Eur. Phys. J. C **84**, no.3, 338 (2024) [erratum: Eur. Phys. J. C **84**, no.5, 454 (2024)] doi:10.1140/epjc/s10052-024-12692-y [arXiv:2312.11427 [hep-ph]].



- [29] D. Jurčiukonis and L. Lavoura, *JHEP* **03** (2022), 106 [arXiv:2107.14207 [hep-ph]].
- [30] W. Grimus and L. Lavoura, *Phys. Rev. D* **66** (2002), 014016 [arXiv:hep-ph/0204070 [hep-ph]].
- [31] M. J. Herrero, X. Marcano, R. Morales and A. Szykman, *Eur. Phys. J. C* **78**, no.10, 815 (2018) doi:10.1140/epjc/s10052-018-6281-3 [arXiv:1807.01698 [hep-ph]].
- [32] P. Abreu *et al.* [DELPHI], *Z. Phys. C* **73**, 243-251 (1997) doi:10.1007/s002880050313
- [33] R. Akers *et al.* [OPAL], *Z. Phys. C* **67**, 555-564 (1995) doi:10.1007/BF01553981
- [34] G. Aad *et al.* [ATLAS], *Phys. Rev. D* **90**, no.7, 072010 (2014) [arXiv:1408.5774 [hep-ex]].
- [35] L. T. Hue, H. T. Hung, N. T. Tham, H. N. Long and T. P. Nguyen, *Phys. Rev. D* **104**, no.3, 033007 (2021) doi:10.1103/PhysRevD.104.033007 [arXiv:2104.01840 [hep-ph]].
- [36] D. Chang and H. N. Long, *Phys. Rev. D* **73**, 053006 (2006) doi:10.1103/PhysRevD.73.053006 [arXiv:hep-ph/0603098 [hep-ph]].
- [37] R. L. Workman *et al.* [Particle Data Group], *PTEP* **2022**, 083C01 (2022) doi:10.1093/ptep/ptac097
- [38] T. P. Nguyen, T. T. Le, T. T. Hong and L. T. Hue, *Phys. Rev. D* **97**, no.7, 073003 (2018) doi:10.1103/PhysRevD.97.073003 [arXiv:1802.00429 [hep-ph]].
- [39] H. K. Dreiner, H. E. Haber and S. P. Martin, *Phys. Rept.* **494**, 1-196 (2010) doi:10.1016/j.physrep.2010.05.002 [arXiv:0812.1594 [hep-ph]].
- [40] L. Ninh and H. N. Long, *Phys. Rev. D* **72**, 075004 (2005) doi:10.1103/PhysRevD.72.075004 [arXiv:hep-ph/0507069 [hep-ph]].
- [41] L. T. Hue, H. N. Long, T. T. Thuc and T. Phong Nguyen, *Nucl. Phys. B* **907**, 37-76 (2016) doi:10.1016/j.nuclphysb.2016.03.034 [arXiv:1512.03266 [hep-ph]].
- [42] V. De Romeri, M. J. Herrero, X. Marcano and F. Scarcella, *Phys. Rev. D* **95** (2017) no.7, 075028 doi:10.1103/PhysRevD.95.075028 [arXiv:1607.05257 [hep-ph]].
- [43] P. A. Zyla *et al.* [Particle Data Group], *PTEP* **2020**, no.8, 083C01 (2020) doi:10.1093/ptep/ptaa104
- [44] K. Abe *et al.* [T2K], *Nature* **580**, no.7803, 339-344 (2020) [erratum: *Nature* **583**, no.7814, E16 (2020)] doi:10.1038/s41586-020-2177-0 [arXiv:1910.03887 [hep-ex]].
- [45] M. Tanabashi *et al.* [Particle Data Group], *Phys. Rev. D* **98**, no.3, 030001 (2018) doi:10.1103/PhysRevD.98.030001
- [46] L. T. Hue, P. N. Thanh and T. D. Tham, *Commun. in Phys.* **30**, no.3, 221-230 (2020) doi:10.15625/0868-3166/30/3/14963